Magnetic order in $Nb_{1-x}Zr_xFe_2$

1996 J. Phys.: Condens. Matter 8 7785

(http://iopscience.iop.org/0953-8984/8/41/022)

J. Phys.: Condens. Matter **8** (1996) 7785–7796. Printed in the UK

Magnetic order in $Nb_{1-x}Zr_xFe_2$

M R Crook†‡, B R Coles‡, C Ritter§ and R Cywinski†‖

† School of Physics and Astronomy, University of St Andrews, St Andrews, Fife KY16 9SS, UK

‡ The Blackett Laboratory, Imperial College of Science and Technology, London SW7 2BZ, UK

§ Institut Laue–Langevin, 38042 Grenoble Cédex, France

Received 28 May 1996, in final form 31 July 1996

Abstract. Neutron powder diffraction has been used to study the evolution of magnetic order with increasing Zr substitution in the C14 Laves phase compounds $Nb_{1-x}Zr_xFe_2$ ($0.18 \leqslant x \leqslant 0.4$). For compounds with $x = 0.3$ and $x = 0.4$ we find a simple antiferromagnetic structure, similar to that reported for isostructural $TiFe_2$. In this structure the Fe moments at the 6h sites are aligned along the *c*-axis, ferromagnetically coupled within the *a*–*b* plane, with adjacent planes antiferromagnetically coupled. This spin structure results in a cancellation of the molecular field at the interplanar 2a sites, and the Fe atoms at these sites carry no ordered moment. The neutron diffraction measurements on $Nb_{1-x}Zr_xFe_2$ compounds in the composition range $0.18 \leqslant x \leqslant 0.22$ provide evidence of a low-temperature spin-canted structure in which the antiferromagnetic structure described above is modified by the appearance of a basal-plane ferromagnetic component which in turn leads to a small ordered Fe moment at the 2a site. The temperature dependence of the staggered magnetization in the antiferromagnetic state of the $x = 0.4$ compounds is found to closely follow the form $M_Q(T) \propto (T_N^{3/2} - T^{3/2})^{1/2}$, as predicted for weak itinerant antiferromagnets by SCR spin-fluctuation theory.

1. Introduction

The C14 hexagonal Laves phase compound $NbFe_2$ exists in a delicately balanced weak magnetic state characterized by a close competition between ferromagnetic and antiferromagnetic spin fluctuations. This delicate balance is easily upset by small changes in composition or by atomic substitution. Stoichiometric $NbFe_2$ is itself a weak itinerant antiferromagnet with a Néel temperature of approximately 18 K. The ground-state spin structure is believed to be of the spin-density-wave type [1]. However, with relatively minor excursions to either Fe-rich or Nb-rich compositions, magnetic order in the $Nb_{1-y}Fe_{2+y}$ compounds evolves via coexisting ferromagnetic and antiferromagnetic phases [2, 3] (for $-0.015 \leqslant y \leqslant +0.015$), to ferromagnetism at higher Fe ($y \geqslant +0.015$) or Nb ($y \leqslant -0.015$) concentrations. On the other hand, substitution for Nb or Zr [4, 5] in the pseudobinary system $Nb_{1-x}Zr_xFe_2$ rapidly stabilizes weak ferromagnetism, with a reversion to antiferromagnetism occurring at a Zr concentration of $x \approx 0.18$. In the antiferromagnetic state the Néel temperature rises rapidly with concentration, reaching room temperature at approximately $x = 0.4$. With further increases in Zr content, near the composition $x = 0.6$, the compounds crystallize with the cubic C15 Laves phase structure rather than with the hexagonal C14 form. Stoichiometric $ZrFe_2$ is a ferromagnet with interesting Invar properties, and a small magnetic moment at the Zr site.

‖ Author to whom any correspondence should be addressed.

0953-8984/96/417785+12$19.50

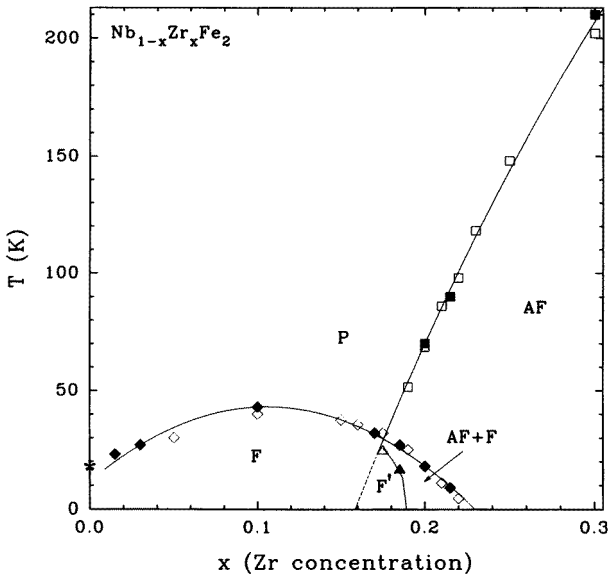

Figure 1. The magnetic phase diagram of $Nb_{1-x}Zr_xFe_2$. Solid symbols are taken from our dc magnetization measurements and hollow symbols are from reference [7]. The asterisk at $x = 0$ indicates the Néel temperature of the spin-density-wave state of stoichiometric $NbFe_2$. (F, F′ = ferromagnetic, AF = antiferromagnetic and P = paramagnetic).

The evolution from weak ferromagnetism to antiferromagnetism in $Nb_{1-x}Zr_xFe_2$ takes place in the composition range $0.16 \leqslant x \leqslant 0.22$, over which it is suggested the ferromagnetic and antiferromagnetic states coexist [5, 6]. In addition, a first-order transition to a second low-temperature ferromagnetic state has been identified [7] in a narrow concentration range centred on approximately $x \approx 0.18$. The magnetic phase diagram of the $Nb_{1-x}Zr_xFe_2$ system, for $0 \leqslant x \leqslant 0.3$, is summarized in figure 1.

Although Mössbauer spectroscopy has been employed [8] in an attempt to determine the spin configurations in antiferromagnetic $Nb_{1-x}Zr_xFe_2$ compounds in the range $0.3 < x < 0.5$, there have, as yet, been no neutron diffraction studies of the evolution of magnetic order in $Nb_{1-x}Zr_xFe_2$ with increasing Zr substitution. In this paper we present the results of such a study of $Nb_{1-x}Zr_xFe_2$ compounds in the antiferromagnetic and coexisting ferro- and antiferromagnetic phases.

2. Sample preparation and experimental details

7 g ingots of $Nb_{1-x}Zr_xFe_2$, with $0.18 \leqslant x \leqslant 0.4$, were prepared by arc melting appropriate quantities of Nb (99.9%), reactor-grade Zr (99.98%) and Fe (99.98%) under an argon atmosphere. To ensure homogeneity the ingots were repeatedly turned and melted. Three separate ingots of each compound were prepared. These were then coarsely crushed and remelted into secondary ingots, each containing equal proportions of the original ingots. Typical mass loss during this process was approximately 0.1% . The secondary ingots were then crushed, yielding approximately 20 g of powder for each neutron diffraction sample.

The neutron diffraction experiments were performed on the POLARIS [9] time-of-flight powder diffractometer at the Rutherford Appleton Laboratory's pulsed spallation neutron

source, ISIS, and on the D1B powder diffractometer at the Institut Laue–Langevin (ILL) high-flux reactor neutron source. For both the POLARIS and D1B experiments powdered samples were contained in a cylindrical vanadium can within a conventional 'orange' cryostat. Measurements on POLARIS were made as a function of temperature between 4 K and 293 K for $Nb_{1-x}Zr_xFe_2$ samples with $x = 0.4$ and for $x = 0.3$ at 293 K and 4 K. On D1B, measurements were made on samples with $x = 0.4, 0.3, 0.22, 0.2$ and 0.18 at several fixed temperatures, including a base temperature of 1.2 K and just above the respective magnetic ordering temperatures (see figure 1).

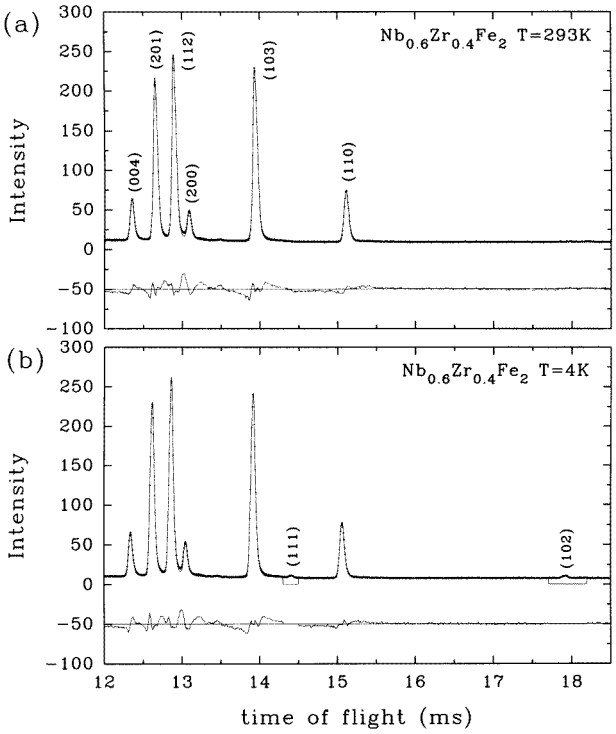

Figure 2. A section of the time-of-flight diffraction patterns, collected using the POLARIS diffractometer, together with the associated CAILS refinements and residuals, for $Nb_{0.6}Zr_{0.4}Fe_2$ at (a) 293 K and at (b) 4 K. The positions of the 'forbidden' (111) peak and the nuclear (102) peak are indicated in (b).

The neutron diffraction spectra obtained on POLARIS were refined using the Pawley-type cell and intensity least-squares [10] (CAILS) refinement routine of the Cambridge Crystallography Subroutine Library. The CAILS routine allows the determination of cell constants, sample-dependent peak-width parameters and integrated peak intensities. The relative integrated peak intensities are not constrained within the CAILS routine, and therefore parameters such as atomic positions and Debye–Waller factors cannot be refined. From the analysis of the spectra it was apparent that the POLARIS samples exhibited considerable preferred orientation.

On D1B, diffraction spectra were collected using a neutron wavelength of 2.52 Å, over an angular range of $12.62^\circ \leqslant 2\theta \leqslant 92.42^\circ$. Full conventional Rietveld refinements of the spectra were performed using the FULLPROF program [11]. The powder samples studied

on D1B were of significantly finer grain size than those used on POLARIS, and no preferred orientation was observed.

Table 1. Crystallographic parameters of the C14 Laves phase structure (space group: $P6_3/mmm$) of $Nb_{1-x}Zr_xFe_2$.

Site	Atom	Atomic positions	
2a	Fe	(0, 0, 0); (0, 0, 1/2)	
6h	Fe	$\pm(x, x, 1/4)$	$x = -1/6$
		$\pm(2x, x, 1/4)$	
		$\pm(x, 2x, 1/4)$	
4f	Nb/Zr	$\pm(1/3, 2/3, z)$	$z = -1/16$
		$\pm(1/2, 2/3, 1/2 - z)$	

3. Experimental results and discussion

3.1. $Nb_{1-x}Zr_xFe_2$ with $x = 0.3$ and $x = 0.4$: the antiferromagnetic state

Figure 2 shows a section of the time-of-flight powder diffraction spectra for the $Nb_{1-x}Zr_xFe_2$ compound with $x = 0.4$ at 4 K and at 293 K, obtained from the high-resolution, high-(backward-) angle detector bank of the POLARIS diffractometer. The corresponding patterns for this compound, at 1.2 K and at 290 K, obtained from the D1B diffractometer are shown in figure 3. The very small peaks in this latter figure, which are not indexed and which were not observed at ISIS, arise from second-order contamination of the monochromatic beam.

At 290 K the spectra are fully consistent with diffraction from a C14 hexagonal Laves phase structure with space group $P6_3/mmc$ (see table 1). Because of the limitations of the CAILS refinement programmes the x-coordinate of the 6h Fe site was fixed at 0.1667, while the z-coordinate of the 4f Nb/Fe sites was fixed at $z = 0.0625$.

Below $T_N \approx 270$ K the compound is found to order antiferromagnetically: an increase in the intensity of some of the Bragg reflections, corresponding to the onset of coherent magnetic scattering, is observed. This is most clearly observed for the (102) reflection, indicated in figure 2(b) and figure 3(b), for which the nuclear structure factor is close to zero. An additional feature is the appearance of a small peak at the (111) position below T_N . Similar differences are also observed between the high- and low-temperature powder diffraction patterns obtained from the $Nb_{1-x}Zr_xFe_2$ compound with $x = 0.3$, which orders antiferromagnetically at $T_N \approx 210$ K.

The superposition of magnetic and nuclear contributions to the Bragg reflections suggests that the magnetic unit cell is commensurate with the chemical unit cell. In addition, for the space group $P6_3/mmc$, reflections of the form (hhl) are allowed only for $l = 2n$. Thus the reflection indexed as (111), i.e. (hhl) with $l =$ odd, is entirely magnetic in origin. We might expect to see other similar families of reflections, in particular the series $(00l)$ with $l =$ odd. However, this family is absent. The clear implication is that the magnetic spins lie along the c-axis.

All of these observations are consistent with the magnetic structure proposed in an earlier analysis of the Mössbauer spectra [8] of $Nb_{1-x}Zr_xFe_2$ and shown in figure 4. The magnetic moments at the Fe 6h sites, which form planar Kagomé nets, are ferromagnetically aligned along the c-direction within the planes whilst adjacent layers are antiferromagnetically

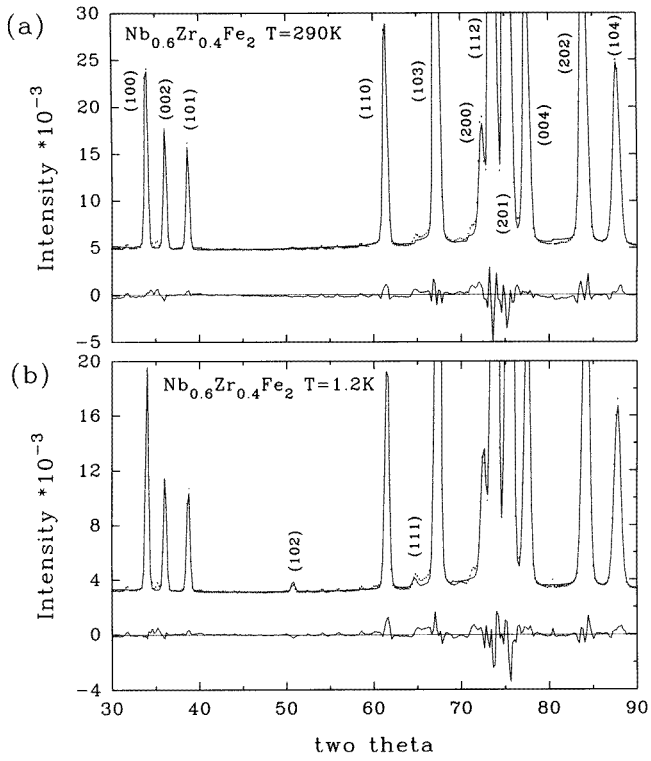

Figure 3. The details of the low-intensity Bragg peaks of the diffraction patterns, obtained on D1B, of $Nb_{0.6}Zr_{0.4}Fe_2$ at (a) 290 K and (b) 1.2 K. The associated (a) nuclear and (b) nuclear plus magnetic Rietveld refinements and residuals obtained using FULLPROF are also shown in the figures as solid lines. In (b) the magnetic contributions at the (102) and (111) positions are evident.

coupled. The Fe 2a sites lie at a position of high magnetic symmetry between the 6h layers and thus have no ordered moment because of the cancellation of the molecular field at this position. It should be noted that the magnetic structure of figure 4 is identical to that previously established from neutron diffraction measurements on the isostructural C14 Laves phase compound, $TiFe_2$ [12].

The D1B diffraction spectra were refined using the full Rietveld method. For the spectrum collected at 1.2 K the magnetic and atomic structures were refined simultaneously. The crystallographic parameters (the lattice parameter, the fractional cell coordinate x, and the temperature factors) common to the magnetic and atomic structures were varied in the refinement, whilst the magnitude of the magnetic moment at the Fe 6h site was the only independent magnetic variable. A summary of the results of the refinements for $Nb_{1-x}Zr_xFe_2$ compounds with $x = 0.3$ and $x = 0.4$ is given in table 2, and the refinements are shown in figure 3. The magnetic moments at the Fe 6h site are found to be $0.73(9)\mu_B$ and $1.13(6)\mu_B$ for the $x = 0.3$ and $x = 0.4$ $Nb_{1-x}Zr_xFe_2$ samples respectively. These moments are considerably lower than the value of $1.4(1)\mu_B$ reported for isostructural $TiFe_2$.

Figure 5(a) shows the variation with temperature of the relative magnetic structure factors, $|F_{100}|$ and $|F_{101}|$, obtained for the (100) and (101) magnetic reflections as observed in the low-angle detector bank of the POLARIS diffractometer. These two strong magnetic

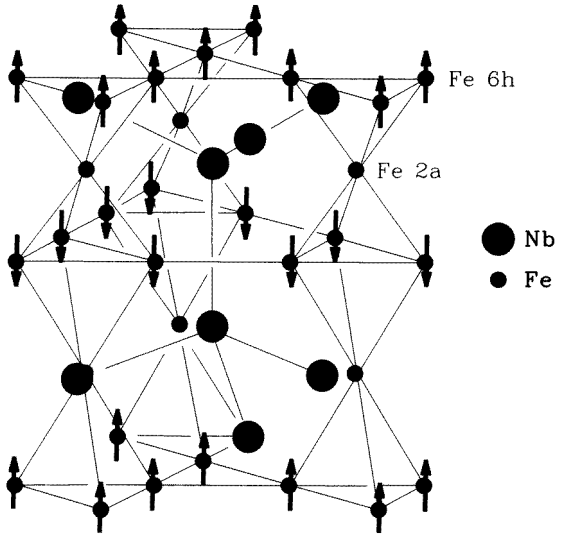

Figure 4. The crystallographic and magnetic structure of $Nb_{1-x}Zr_xFe_2$ in the simple collinear antiferromagnetic region of the magnetic phase diagram ($0.2 \leqslant x \leqslant 0.6$).

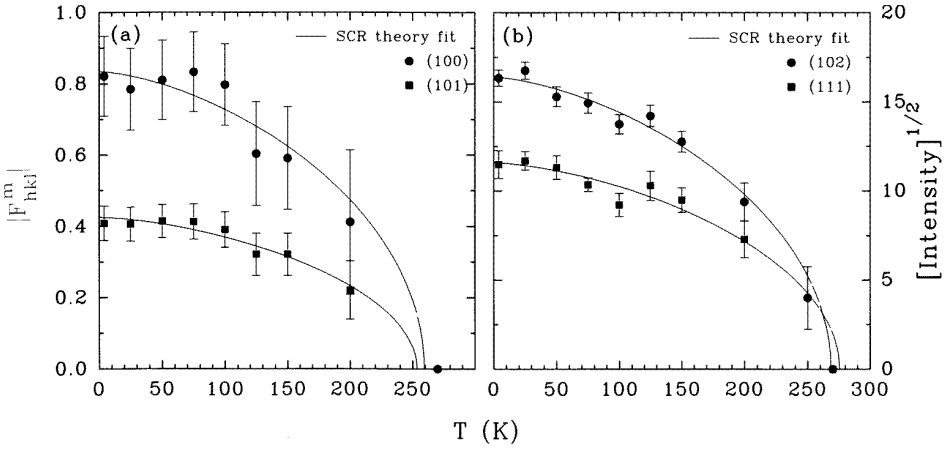

Figure 5. The temperature dependence of (a) the magnetic structure factors of the (100) and (101) magnetic reflections and (b) the intensities of the (102) and (111) magnetic reflections from $Nb_{0.6}Zr_{0.4}Fe_2$ measured on POLARIS. The solid lines represent a least-squares fit of the SCR expression for the staggered magnetization of weak itinerant antiferromagnets (see the text).

reflections are superimposed upon their corresponding nuclear reflections and are positioned at either side of the purely nuclear (002) reflection. The CAILS program gives the intensity, I, of each reflection, (hkl), in the form

$$I = K(\lambda, \theta) m_{hkl} |F_{hkl}|^2 \exp\{-2W\}$$

where $|F_{hkl}|^2$ is the square of the structure factor, m_{hkl} is the multiplicity of the reflection. $K(\lambda, \theta)$ represents the geometrical contribution to the measured intensities and $\exp\{-2W\}$

Table 2. A summary of the D1B profile refinements for $Nb_{1-x}Zr_xFe_2$, with $x = 0.3, 0.4$.

x	T (K)	R-factors	a, c (Å)	Cell coordinates	Moment (μ_B)
0.4	290	R_p 5.07	a 4.8913(3)	z (4a) 0.0649(3)	—
		R_{wp} 5.41	c 7.9965(6)	x (6h) ±0.1697(3)	
		R_B 2.47			
	1.2	R_p 4.97	a 4.8788(3)	z (4a) 0.0650(3)	m_z ±1.13(6)
		R_{wp} 5.28	c 7.9924(5)	x (6h) ±0.1699(3)	
		R_B 2.11			
		Magnetic 6.42 *(collinear AF)*			
0.3	240	R_p 4.68	a 4.8689(3)	z (4a) 0.0631(3)	—
		R_{wp} 5.17	c 7.9587(5)	x (6h) ±0.1692(3)	
		R_B 2.25			
	1.2	R_p 4.40	a 4.8600(3)	z (4a) 0.0632(3)	m_z ±0.73(9)
		R_{wp} 5.01	c 7.9536(5)	x (6h) ±0.1693(3)	
		R_B 1.83			
		Magnetic 8.31 *(collinear AF)*			

is the Debye–Waller factor. The relative squared magnetic structure factors, $|F^m_{hkl}|^2$, were extracted from the total structure factor $|F_{hkl}|^2$ by subtracting the nuclear structure factor, $|F^n_{hkl}|^2$, obtained from measurements above T_N, according to

$$|F^m_{hkl}|^2 = (m^n_{hkl}/m^m_{hkl})(|F_{hkl}|^2 - |F^n_{hkl}|^2)$$

with the total structure factor calculated from the intensity of the combined nuclear plus magnetic line by ascribing the nuclear multiplicity, m^n_{hkl}, to this combined line. The temperature dependence of $|F^n_{002}|^2$, for the purely nuclear (002) peak, was used to make a small Debye–Waller correction, assuming that the dependence Q ($=4\pi \sin\theta/\lambda$) of W may be neglected since the (100), (002) and (101) peaks are adjacent in Q. In addition we have used the ratio of the calculated values of $|F^n_{hkl}|^2$, to the measured values, provided by the CAILS routine, to determine a preferred orientation correction for the (100) and (101) reflections. A similar normalization and correction of the magnetic structure factors of the (111) and (102) reflections was precluded as the equivalent nuclear reflections are 'forbidden'. In figure 5(b) we therefore present the temperature variation of the square-root intensities.

Moriya's self-consistent renormalization (SCR) theory of spin fluctuations [13] predicts that the temperature dependence of the staggered magnetization of weak itinerant antiferromagnets takes the form

$$M_Q(T) \propto (T_N^{3/2} - T^{3/2})^{1/2}.$$

The lines in figure 5(a) are least-squares fits of this functional form to the magnetic structure factors of the (100) and (101) magnetic reflections, and those in figure 5(b) are those to the square roots of the intensities of the (102) and (111) magnetic reflections. Although the least-squares fits were not constrained to pass through the Néel temperature, T_N was included in the data as a point of zero intensity. As can be seen the agreement with the predictions of SCR theory is reasonable, particularly for the (111) and (102) reflections for which corrections for the underlying nuclear reflections were unnecessary.

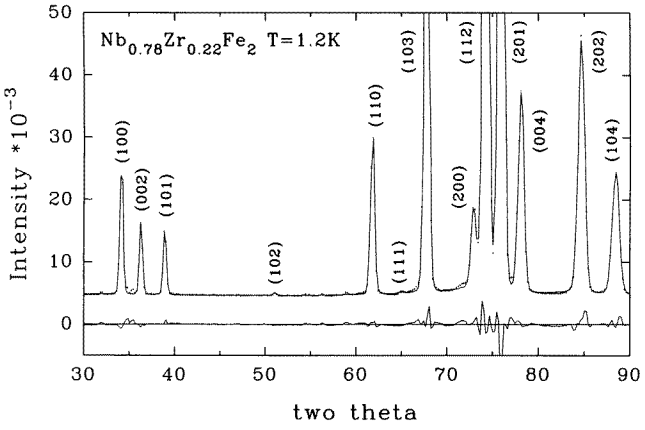

Figure 6. The diffraction pattern of $Nb_{0.78}Zr_{0.22}Fe_2$ at 1.2 K collected on D1B, shown together with the full (magnetic plus nuclear) profile refinement and residuals. The magnetic structure is assumed to be the spin-canted modification to the collinear spin structure shown in figure 4.

Table 3. Diffraction pattern peak intensities from $Nb_{1-x}Zr_xFe_2$, with $x = 0.22, 0.2$ and 0.18.

Peak	Temperature*	$I(x = 0.22)$	$I(x = 0.2)$	$I(x = 0.18)$
(100)	H	87 420(204)	181 372(299)	
	M	88 916(177)	183 069(299)	262 640(508)
	L	89 050(203)	183 412(199)	263 103(503)
(002)	H	48 439(199)	106 405(281)	
	M	48 473(173)	106 825(282)	138 353(471)
	L	48 440(199)	108 036(281)	143 283(623)
(101)	H	45 795(178)	99 866(274)	
	M	46 616(153)	101 147(275)	139 684(313)
	L	46 917(176)	101 326(274)	140 732(348)
(102)	H	small	1890(79)	
	M	1152(47)	2454(82)	2366(158)
	L	1536(44)	2681(47)	2881(135)
(110)	H	145 043(373)	307 428(705)	
	M	145 391(364)	308 299(670)	415 557(1063)
	L	146 191(359)	308 271(736)	417 489(901)
(103)	M			1 483 301(1248)
	L			1 486 748(1297)
(202)	M			1 065 638(3905)
	L			1 066 049(3886)

*The temperatures H = high, M = medium and L = low refer to 110 K, 50 K and 1.2 K for $x = 0.22$, 80 K, 35 K and 1.2 K for $x = 0.2$ and 37.5 K and 1.2 K for $x = 0.18$ respectively.

3.2. $Nb_{1-x}Zr_xFe_2$ with $x = 0.2$ and $x = 0.22$: the mixed magnetic state

The magnetic phase diagram of $Nb_{1-x}Zr_xFe_2$ compounds in this composition range suggests a complex interplay between ferromagnetic and antiferromagnetic ground states. For

example, the compounds with $x = 0.22$ ($T_N \approx 100$ K) and $x = 0.2$ ($T_N \approx 70$ K) undergo transitions from the antiferromagnetic to coexisting ferromagnetic plus antiferromagnetic states at $T_{C1} = 5$ K and $T_{C1} = 20$ K respectively (figure 1).

Neutron diffraction spectra of $Nb_{1-x}Zr_xFe_2$ compounds were collected on D1B at temperatures of 110 K, 50 K and 1.2 K for $x = 0.22$, at 80 K, 35 K and 1.2 K for $x = 0.2$ and at 37.5 K and 1.2 K for $x = 0.18$ (see figure 1). A typical diffraction pattern, i.e. that of the $x = 0.22$ sample at 1.2 K, is illustrated in figure 6. A summary of the diffraction measurements is given in table 3, where the integrated intensities of individual diffraction peaks are listed for each compound at each temperature. The integrated intensities were obtained from least-squares fits of gaussian profiles to those peaks which could be individually resolved.

For the $x = 0.22$ sample the differences between the peak intensities at 110 K and 50 K are consistent with the transition, at $T_N \approx 100$ K, from a paramagnetic state to an antiferromagnetic state. This is most clearly seen as an increase in intensity of 1.7(2)% and 1.8(4)% for the (100) and (101) reflections respectively and, in addition, from the emergence of a small magnetic peak at the position of the negligible nuclear (102) reflection. The 'forbidden' (111) reflection also appears in the 50 K spectrum, although an accurate estimation of the intensity of this peak was not possible. These results, together with the observation that there is no magnetic contribution to the intensity of the (002) reflection, indicates that the antiferromagnetic structure at 50 K is consistent with that determined for the $x = 0.3$ and $x = 0.4$ samples below their respective Néel points and shown in figure 4. Similar changes in the diffraction pattern of the $x = 0.20$ sample between 80 K and 35 K also indicate the onset of the same antiferromagnetic structure. For this compound the intensities of the (100) and (101) reflections increase by 0.94(2)% and 1.3(3)% respectively and magnetic intensity appears at (102) and (111), while the intensity of the (002) reflection remains constant.

On cooling the $x = 0.22$ compound to 1.2 K the magnetic intensity of the (102) reflection is seen to increase further, while that of the (002) reflection remains constant. Cooling the $x = 0.2$ compound to 1.2 K results in a similar increases in the intensities of the magnetic (102) reflection, although in this case there is a significant increase of 1.13(26)% in the intensity of the (002) reflection.

For the simple collinear spin structure shown in figure 4 no magnetic contribution to the (002) reflection is expected. The appearance of magnetic diffraction intensity at this position in the low-temperature (1.2 K) diffraction spectrum of the $x = 0.2$ compound is therefore a clear indication of a spin component orthogonal to the c-axis. Indeed NMR measurements [6] have previously indicated a canted arrangement for the low-temperature spin structure of $Nb_{1-x}Zr_xFe_2$ compounds at these intermediate compositions. It has been further suggested [6] that a ferromagnetic component lies in the basal plane while the antiferromagnetic component remains parallel to the c-axis. The appearance of the (002) magnetic reflection in the 1.2 K spectrum of the $x = 0.2$ compound is fully consistent with the developing basal-plane magnetization component of this spin-canted arrangement. Moreover, it is probable that the observed basal-plane component is related to a ferromagnetic component of the magnetization: the extreme topological frustration associated with the stabilization of antiferromagnetic correlations within the 2d triangular lattice formed by the Fe 6h sites in the basal plane is likely to constrain any antiferromagnetic component of magnetization to the c-axis. It should also be noted that the appearance of a basal-plane ferromagnetic component will lead to a finite molecular field at the 2a Fe site. An ordered Fe moment might therefore be expected at the 2a site in the spin-canted phase.

Although a similar spin structure might be expected for the $x = 0.22$ compound, it

Table 4. A summary of the D1B profile refinements for $Nb_{1-x}Zr_xFe_2$, with $x = 0.22$ and 0.2.

x	T (K)	R-factors	a, c (Å)	Cell coordinates	Moment (μ_B)
0.22	110	R_p 5.17 R_{wp} 5.83 R_B 1.12	a 4.8565(3) c 7.9378(6)	z (4a) 0.0639(3) x (6h) ±0.1693(3)	—
	50	R_p 4.89 R_{wp} 5.70 R_B 2.26 Magnetic 4.56 *(collinear AF)*	a 4.8551(3) c 7.9374(5)	z (4a) 0.0639 x (6h) ±0.1693	m_z ±0.74(8)
	1.2	R_p 5.03 R_{wp} 5.76 R_B 2.32 Magnetic 5.87 *(collinear AF)*	a 4.8549(3) c 7.9378(5)	z (4a) 0.0639 x (6h) ±0.1693	m_z ±0.76(8)
0.20	80	R_p 5.11 R_{wp} 5.12 R_B 3.76	a 4.8481(3) c 7.9233(6)	z (4a) 0.0634(3) x (6h) ±0.1695(3)	—
	35	R_p 5.26 R_{wp} 5.83 R_B 2.34 Magnetic 9.19 *(collinear AF)*	a 4.8473(3) c 7.9232(5)	z (4a) 0.0634 x (6h) ±0.1695	m_z ±0.55(10)
	1.2	R_p 5.25 R_{wp} 5.84 R_B 2.31 Magnetic 6.38 *(canted AF)*	a 4.8571(3) c 7.9232(5)	z (4a) 0.0634 x (6h) ±0.1695	m_z ±0.55(10) m_x 0.2(1)
	1.2	Magnetic 8.73 *(collinear AF)*			m_z ±0.53(11)

has not been possible to detect any changes to the spin arrangement on cooling below $T_{C1} = 5$ K. It is likely that in this case the low-temperature ferromagnetic component in the basal plane is too small to be observed on D1B.

Table 4 summarizes the profile refinements of the diffraction patterns of the $x = 0.22$ and $x = 0.20$ compounds both above and below their respective ordering temperatures. For $x = 0.22$, at 50 K and 1.2 K, and for $x = 0.2$, at 35 K and 1.2 K the magnetic refinements have been performed assuming the collinear antiferromagnetic spin structure illustrated in figure 4. In addition the diffraction pattern from the $x = 0.2$ compound at 1.2 K has been refined using the suggested spin-canted spin modification to the collinear structure, within which a small ferromagnetic component of magnetization is allowed to develop on *both* the Fe 6h and 2a sites within the basal plane. The resulting improvement to the magnetic R-factor suggests that the spin-canted structure is a better representation of the low-temperature magnetic ground state.

3.3. $Nb_{1-x}Zr_xFe_2$ with $x = 0.18$: the re-entrant magnetic state

According to the phase diagram of figure 1, the $Nb_{1-x}Zr_xFe_2$ compound with $x = 0.18$ has a Néel point of $T_N \approx 35$ K and a transition to the mixed magnetic phase at $T_{C1} \approx 27$ K. There follows a further, re-entrant, transition, at $T_{C2} \approx 20$ K, to ferromagnetic order. However, our magnetization measurements on this sample indicate an ordered moment of only $0.1\mu_B$ per Fe atom in the low-temperature ferromagnetic state. Such small moments

Table 5. A summary of the magnetic profile refinements for $Nb_{1-x}Zr_xFe_2$.

x	T (K)	R-factor	Moment (μ_B)
0.4	1.2	6.42	m_z ±1.13(6)
0.3	1.2	8.31	m_z ±0.73(9)
0.22	50	4.56	m_z ±0.74(8)
	1.2	5.87	m_z ±0.76(8)
0.2	35	9.19	m_z ±0.55(10)
	1.2	6.38	m_z ±0.55(10), m_x ±0.2(1)

are strictly beyond the limits of sensitivity of the D1B diffractometer. The paucity of systematic intensity differences between the low- and high-temperature spectra precludes a determination of the spin structure at this composition. However, as can be seen in table 2, there are small increases in the intensities of the (002) and (102) Bragg reflections on cooling from 37.5 K to 1.2 K. The magnetic intensity of the (002) Bragg reflection suggests that a significant component of the magnetization lies in the basal plane.

4. Conclusions

The neutron diffraction experiments described here have provided the first direct observation of the spin structure in the antiferromagnetic region, $0.2 < x < 0.6$, of the $Nb_{1-x}Zr_xFe_2$ magnetic phase diagram. At the higher concentrations ($x = 0.3, 0.4$) these observations are fully consistent with the results of previous Mössbauer spectroscopy measurements [8], and also with the spin structure proposed for the related C14 Laves phase compound, $TiFe_2$ [12]. At lower concentrations ($x = 0.2$) there is considerable evidence for a spin-canted modification to the simple collinear antiferromagnetic structure in the low-temperature region for which a coexistence of ferromagnetic and antiferromagnetic states has been previously proposed.

A summary of the magnetic structures obtained from a Rietveld refinement of the neutron diffraction spectra is given in table 5. In the collinear antiferromagnetic phase the magnitude of the ordered Fe moment at the 6h site is found to decrease from approximately $1.1\mu_B$ to $0.58\mu_B$ as the Zr concentration is reduced from $x = 0.4$ to $x = 0.2$. These values are comparable to those determined from NMR measurements [5, 6]. However, in the low-temperature spin-canted phase of the $x = 0.2$ compound we estimate an additional basal-plane ferromagnetic component of magnetization of $0.2\mu_B$, somewhat larger than the value of $0.05\mu_B$ suggested by NMR [6]. The absence of an ordered magnetic moment at the 2a site in the collinear antiferromagnetic state of $Nb_{1-x}Zr_xFe_2$ is of particular interest. It not possible to ascertain from the present measurements whether the Fe atoms at this site are non-magnetic or simply magnetically disordered. However, the situation in $Nb_{1-x}Zr_xFe_2$ is perhaps analogous to that in the related C14 compound, $TiFe_2$, for which polarized neutron measurements have established that Fe atoms at the 2a site carry no moment [12].

The absence of a moment at the Fe 2a site in $TiFe_2$ is interpreted as evidence that the essentially itinerant Fe moments are close to a magnetic instability. In the case of $Nb_{1-x}Zr_xFe_2$ the itinerant character of the Fe moments is further emphasized by the temperature dependence of the staggered magnetization of the $x = 0.4$ compound which closely follows the form predicted by the SCR theory [13] of weak itinerant antiferromagnetism. SCR theory, however, is generally applicable only in the limit of weakly localized moments, such as those observed in vanadium chalcogenides, for which

the Néel temperatures are typically 15 K, and the ordered moments $0.1\mu_B$ [14]. It is therefore surprising that SCR theory describes the temperature dependence of the staggered magnetization of $Nb_{0.6}Zr_{0.4}Fe_2$ so precisely, since the relatively large ordered Fe moment ($1.13\mu_B$) and high Néel temperatures (200–300 K) should place this compound outside the weak itinerant limit.

Acknowledgments

BRC and RC gratefully acknowledge financial support from the Engineering and Physical Sciences Research Council. MRC acknowledges the receipt of an EPSRC research studentship. The authors would also like to thank Dr R I Smith of ISIS for assistance with the POLARIS experiments.

References

[1] Yamada Y, Nakamura H, Kitaoka Y, Asayama K, Koga K, Sakata A and Murakami T 1990 *J. Phys. Soc. Japan* **59** 2967
[2] Crook M R and Cywinski R 1995 *J. Magn. Magn. Mater.* **140–144** 71
[3] Shiga M and Nakamura Y 1987 *J. Phys. Soc. Japan* **56** 4040
[4] Yamada Y and Ohira K 1983 *J. Phys. Soc. Japan* **52** 3646
[5] Yamada Y, Kitaoka Y, Asayama K and Sakata A 1984 *J. Phys. Soc. Japan* **53** 3198
[6] Yamada Y, Kitaoka Y, Asayama K and Sakata A 1984 *J. Phys. Soc. Japan* **53** 3634
[7] Yamada Y, Kitaoka Y, Asayama K, Sakata A and Murakami T 1987 *J. Magn. Magn. Mater.* **70** 175
[8] Nakamura Y and Shiga M 1980 *J. Magn. Magn. Mater.* **15–18** 629
[9] Hull S, Smith R I, David W I F, Hannon A C, Mayers J and Cywinski R 1992 *Physica* B **180+181** 1000
[10] David W I F, Ibberson R M and Matthewman J C 1992 *Rutherford Appleton Laboratory Report* RAL-92-032
[11] Rodriguez J, Anne M and Pannetier J 1987 *Institut Laue–Langevin Report* 87R014T
[12] Brown P J, Deportes J and Ouladdiaf B 1992 *J. Phys.: Condens. Matter* **4** 10 015
[13] Hasegawa H and Moriya T 1974 *J. Phys. Soc. Japan* **36** 1542
[14] Kitaoka Y, Yasuoka H, Oka K, Kosuge K and Kachi S 1979 *J. Phys. Soc. Japan* **46** 1381